

# Highly Electrophilic Titania Hole as a Versatile and Efficient Photochemical Free Radical Source

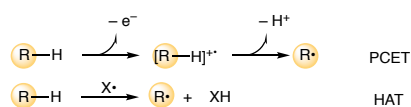
Andrew Hainer<sup>†</sup>, Nancy Marina<sup>†</sup>, Stefanie Rincon, Paolo Costa, Anabel E. Lanterna<sup>\*</sup> and Juan C. Scaiano<sup>\*</sup>

Department of Chemistry and Biomolecular Sciences and Centre for Advanced Materials Research (CAMaR), University of Ottawa, Ottawa, Canada K1N 6N5

Supporting Information Placeholder

**ABSTRACT:** Photogenerated holes in nanometric semiconductors, such as TiO<sub>2</sub>, constitute remarkable powerful electrophilic centers, capable of capturing an electron from numerous donors such as ethers, or non-activated substrates like toluene or acetonitrile, and constitute an exceptionally clean and efficient source of free radicals. In contrast with typical free radical precursors, semiconductors generate single radicals (rather than pairs), where the precursors can be readily removed by filtration or centrifugation after use, thus making it a convenient tool in organic chemistry. The process can be described as an example of dystonic proton coupled electron transfer (PCET).

C–H activation has gained much interest due to its atom and step-economy in the synthesis of functional molecules,<sup>1</sup> many of them are of importance in drug development. Among these, the sp<sup>3</sup> α-C–H reactions of heteroatomic compounds (e.g., alcohols, ethers, or amines) have particular synthetic value as they can directly introduce active groups.<sup>2</sup> For example, the THF motif ranks 11 among the 100 most frequently used ring systems from small molecule drugs listed by FDA,<sup>3</sup> and is part of eribulin and afatinib, two commercial cancer treatment drugs.<sup>4</sup> Thus, the study of different methodologies to couple this and other structures to organic molecules has gained much attention.<sup>5</sup> Two mechanisms proposed for radical C–H activation, involve the cleavage of a C–H bond by hydrogen atom transfer (HAT) or a single-electron transfer, usually coupled to proton loss, described as proton coupled electron transfer (PCET),<sup>6</sup> Scheme 1.

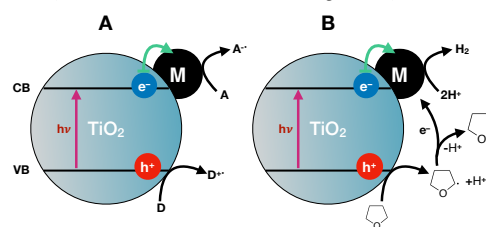


**Scheme 1. C–H activation via HAT and PCET.**

These mechanisms normally require the presence of a free radical initiator that generates two radicals, leaving initiator-

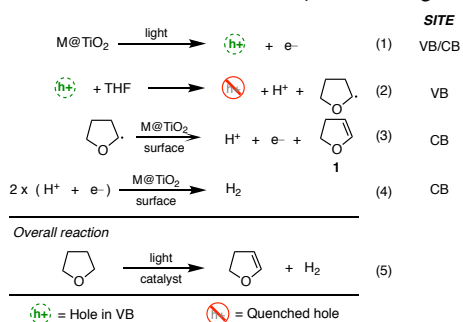
derived debris in the solution along with residual initiator, which can be difficult to remove. Here, we demonstrate that photoactivated TiO<sub>2</sub> can be used as a clean free radical initiator, circumventing some of the disadvantages mentioned.

Many of the studies involving TiO<sub>2</sub> radical formation deal with the generation of reactive oxygen species (ROS), whose involvement ranges from applications in environmental remediation<sup>7</sup> to potential concerns when ROS are used in sunscreens.<sup>8</sup> In contrast, our report is focused on the clean formation of free carbon-centered radicals for applications in organic chemistry. Two recent examples show that semiconductor-based photocatalysts can activate THF, ultimately leading to C–C coupling reactions.<sup>9</sup> Here, we explore in detail the initiation reaction with various substrates. While ethers are not very good electron donors (for example, they show a broad electrochemical window)<sup>10</sup>, it is remarkable that the photogenerated TiO<sub>2</sub>-hole is so electrophilic that it readily oxidizes ethers. Indeed, it can also oxidize non-activated substrates such as toluene and acetonitrile. While most initiators generate a pair of free radicals, TiO<sub>2</sub> makes a single radical – therefore, cage recombination is not an issue. Further, residual TiO<sub>2</sub> and any H<sub>2</sub> produced are readily removed. While the key reaction occurs at the hole (Scheme 2), the electron-hole recombination can be slowed down by decorating TiO<sub>2</sub> with metal nanoparticles, one of the strategies explored here.



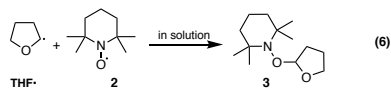
**Scheme 2. A) Metal nanoparticles improve charge separation in TiO<sub>2</sub> semiconductors facilitating both, reduction (A→A<sup>•+</sup>) and oxidation (D→D<sup>•+</sup>) pathways. B) Proposed mechanism for ethers (illustrated for THF).**

Our experiments use 368 nm LED irradiation of metal decorated TiO<sub>2</sub>, such as Pd@TiO<sub>2</sub>, suspended in the reaction mixture. While our work concentrates on organic solvents, the reaction is also water-tolerant (Fig. S2). The photolysis generates H<sub>2</sub> gas as a by-product, just as many sacrificial electron donors do.<sup>11</sup> This gives the system the ability to remove H<sup>+</sup> from solution, making base unnecessary for reactions that can withstand mild acidic conditions. Scheme 3 shows our proposed mechanism, where we anticipate that the hole will reside in the TiO<sub>2</sub> valence band (VB), while the electrons will migrate rapidly to the metal particle, effectively their host. Dihydrofuran and furan were detected by NMR (Fig S11-S12).



**Scheme 3: Mechanism for the formation of H<sub>2</sub> and dihydrofuran from THF. THF-derived radicals (eq. 2) are mobile and undergo solution reactions.**

The generation of radicals does not guarantee they are “free”, in the sense that they are mobile and can participate in solution reactions, as in some cases surface-generated intermediates can remain and react on the surface. In order to validate the mechanism and evaluate if the THF radical is truly free, we used TEMPO (2) as a free radical scavenger. Reaction 6 illustrates the process, where the product can be readily detected by gas chromatography.



Product 3 is formed quantitatively in the presence of TEMPO and different M@TiO<sub>2</sub> nanocomposites (Fig. 1). In order to establish how efficient the process was, we examined eight different catalysts, including bare TiO<sub>2</sub>. Most of these materials were used in earlier reports and their properties are summarized in Table S1. We monitored the time required for 50% of the TEMPO to yield radical trapping products upon UV irradiation (Fig. S1). Fig. 1A shows a summary of the results, where all decorated materials show similar performance, and are about five times more efficient than bare TiO<sub>2</sub>. This virtual independence of the electron trapping material supports the TiO<sub>2</sub> hole as responsible for the electrophilic properties observed. It is clear that the dominant feature of these materials is that surface metals (or their oxides) can greatly increase the longevity of hole-electron pair, slowing down charge recombination and favoring trapping by molecules in the medium, such as THF in these examples.

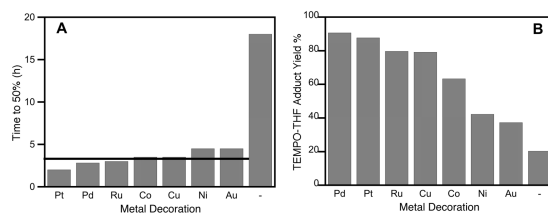


**Figure 1. A: Time for 50% TEMPO to product 3 conversion under 368 nm irradiation. Horizontal line at 3.4 h represents average time for all M@TiO<sub>2</sub> samples. Full kinetic details in Fig. S1. B: Yield of product 3 using various M@TiO<sub>2</sub>. Conditions: 5 mL THF, 25 mM TEMPO, 25 mM Cs<sub>2</sub>CO<sub>3</sub>, 20 mg catalyst, Ar, hν at 2500 Wm<sup>-2</sup>, 4 h.**

The formation of H<sub>2</sub> (eq. 4-5) was followed in the absence and in the presence of TEMPO. As illustrated in Fig. 2, H<sub>2</sub> production is significantly reduced when TEMPO is present. This is consistent with generation of conduction band (CB) electrons by photoexcitation of the semiconductor, while the secondary source of electrons, eq. 3, is inhibited in favor of scavenging by reaction 6. TEMPO trapping supports that the THF radical is free, and thus available for organic chemistry transformations in which it may participate; of course, reaction 6 provides one such a demonstration.

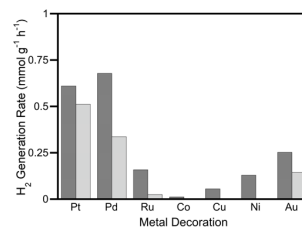


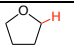
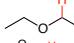
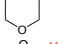
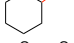
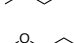
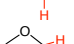
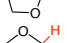
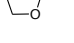
**Figure 2. Rates of photocatalytic H<sub>2</sub> generation for M@TiO<sub>2</sub> in the absence (black) and in the presence of TEMPO (grey). Reaction conditions as in Fig. 1.**

For catalysts such as Ru, Ni, Cu, or Co-decorated TiO<sub>2</sub>, the decorating structures are redox-active oxides that can find alternate pathways for CB electrons,<sup>12</sup> not surprisingly affecting the reducing ability of the material (i.e., H<sub>2</sub> formation). Similarly for cobalt, minor redox changes can affect extensively the outcome of the catalytic process.<sup>13</sup>

Having established that the THF reactivity of various M@TiO<sub>2</sub> is similar among the materials tested, we explored a series of ethers to evaluate the generality of this approach. Note that ethers are known to react rapidly with alkoxy radicals, another highly electrophilic species.<sup>14</sup> The reaction responds to stereoelectronic effects and THF is one of the fastest reactants towards *tert*-butoxy radicals. Our selection of ethers parallels the most interesting examples found for *tert*-butoxy.<sup>14</sup> We have also observed that H<sub>2</sub> is an excellent way to screen for hole-electron reactivity, even if H<sub>2</sub> is derived from CB reactions (eq. 3 and 4).<sup>15</sup> Table 1 summarizes the TEMPO-ether adduct formation for a series of ethers tested, and the H<sub>2</sub> evolution in the absence of TEMPO. Given that many organic reactions are performed in the presence of base, we tested the TiO<sub>2</sub> strategy under these conditions and

140 conclude that the system is base-tolerant; indeed, TEMPO-ether adduct yields are slightly higher in basic media (Table S2), likely due to the decrease of TEMPO-side reactions.<sup>16</sup>

**Table 1. Yields of TEMPO-ether adducts using Pd@TiO<sub>2</sub> photocatalyst and H<sub>2</sub> evolution in the absence of TEMPO**

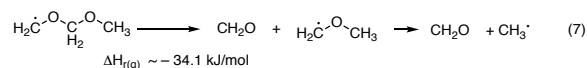
Ether (label)	Structure	TEMPO-Ether Adduct Yield % <sup>a</sup>	H <sub>2</sub> (mmol g <sup>-1</sup> h <sup>-1</sup> )
THF		63.5	0.74
DEE		62.8	0.51
DOX		39.2	0.52
THP		28.2	0.72
DMM		ND	1.32
MOP		ND	1.14
DOL		ND	1.03
MDOL		ND	0.70
No ether		--	0.0

145 Ethers: THF (tetrahydrofuran), DEE (diethyl ether), DOX (dioxane), THP (tetrahydropyran), MOP (1-methoxypropane), DOL (1,3-dioxolane), MDOL (2-methyl-1,3-dioxolane), and DMM (dimethoxymethane). <sup>a</sup>Reaction conditions summarized in SI. Full conversion of TEMPO was obtained in all cases.

150 While TEMPO trapping works very well with THF and other molecules (e.g., dioxane), the product mixture can be complicated by side reactions in other systems, including some cases where the amine 2,2,6,6-tetramethylpiperidine is produced; TEMPO deoxygenation was reported<sup>16</sup> and has been identified in other systems (see SI).

155 In many cases, H<sub>2</sub> generation can be used to screen which ethers are good candidates as hole scavengers (Table 1). Interestingly, among the ethers studied the highest production of H<sub>2</sub> was detected with some that did not show the formation of a stable TEMPO-ether adduct (i.e., DMM, MOP, DOL, and MDOL). This behavior can be rationalized by understanding the chemistry of the radicals. After radical formation these ethers can break the C–O bond to generate the corresponding aldehyde and the carbon-centered radical, where aldehydes, in particular formaldehyde, are great SED for the generation of H<sub>2</sub>. In order to test this hypothesis, we monitored the formation of CH<sub>2</sub>O for the systems where this product is anticipated (i.e., DMM and MOP) and using THF as a (negative) control. Reaction 7 illustrates the cleavage for the radicals derived from DMM, and the corresponding enthalpy of reaction estimated from known thermodynamic data (Scheme S1).<sup>17</sup> In fact, CH<sub>2</sub>O can be detected during the early stages of reaction, and quickly reaches a plateau at 8-10 mM, attributed to the fact that CH<sub>2</sub>O is an excellent SED, quickly reaching steady state concentration when it is consumed as fast as it is generated. Initial formaldehyde formation can be observed with an increasing rate of H<sub>2</sub> generation within the first 15 min of the reaction (Fig. S4). Thus, H<sub>2</sub>

formation is a good reporter for hole trapping even when TEMPO trapping fails due to product mix complexity.



185 Further confirmation that the radicals are free and mobile was obtained by EPR spectroscopy (Fig. S5-S7) and in experiments with THF and dioxane, separate or in equimolar mixtures, where radical recombination products are easily observed, including the cross dimer in the case of solvent mixtures (Fig. S8-S10). In order to compare ether reactivities we also performed a few competitive studies between THF and two other ethers, that presented uncomplicated chemistry in TEMPO trapping studies (Table S3). Whereas the Bu<sup>t</sup>O<sup>•</sup> chemistry relies in stereoelectronic control, this is lost in the TiO<sub>2</sub>-hole chemistry. In the context of Table S3, Bu<sup>t</sup>O<sup>•</sup> is closer to a HAT mechanism, while PCET probably dominates the TiO<sub>2</sub> chemistry. These results combine ether-hole reactivities with surface preference affinities. Computational studies suggest that while dioxane has a modest reactivity, it does have the highest surface affinity. In mix reagents this can lower the relative production of THF radicals in the presence of dioxane due to competition for the reactive surface.

200 To explore further the PCET process, we performed DFT calculations with Quantum Espresso (QE), a package for computing the properties of periodic systems.<sup>18</sup> Association energy ( $E_{\text{ads}}$ ) between substrates and solid surfaces is a computational routine in the QE package. Thus, we computed the energy released by the interaction between THF and TiO<sub>2</sub> (101) anatase surface, under both conditions neutral or positively charged TiO<sub>2</sub> surface. As metals show limited influence on the reactivity of the hole (Fig. 1), only the TiO<sub>2</sub> surface was included in this approximation. Fig. 3 shows top and side view for a THF adsorbed on neutral TiO<sub>2</sub>. A similar configuration is computed for positively charged TiO<sub>2</sub>. Importantly, when the surface is positive the stabilization increases by 23.8 kcal/mol. As the positive surface is a reasonable model for the TiO<sub>2</sub>-hole, this indicates the beginning of the electron transfer process in which THF neutralizes the highly electrophilic hole. In polar media, this becomes the nascent PCET process in which the electron is donated to the hole and the proton stabilized by the solvent, a type of PCET described as dystonic to emphasize the different destination of proton and electron. As expected by their molecular geometry, di-ethers do not show any preferred adsorption configuration compared to those with one oxygen (Fig. S13). Further thermodynamic details can be found in table S4.

225 Free radical formation for other non-activated C–H systems was also shown with pure toluene or acetonitrile. For toluene Fig. S14 shows the formation of bibenzyl and ring coupling products from benzyl radicals. TEMPO also traps <sup>•</sup>CH<sub>2</sub>CN from acetonitrile (Fig. S15). Although the C–H bond dissociation energy (BDE) in acetonitrile (92 kcal/mol<sup>19</sup>) is within the same range of BDE in toluene or  $\alpha$ -

C-H in ethers, this result is appealing as the electron poor nature of CH<sub>3</sub>CN makes it rather inert to typical electrophilic radicals,<sup>20</sup> such as <sup>t</sup>BuO<sup>•</sup>.

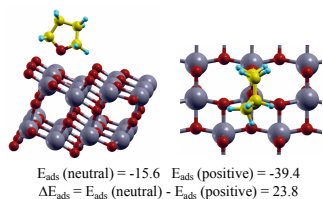


**Figure 3: Computed adsorption configuration of THF on anatase TiO<sub>2</sub> (101) surface. Side (left) and top view.**

In conclusion, hole trapping in TiO<sub>2</sub>, and probably in other semiconductors of comparable band gap, serves as an excellent free radical source, easy to control, use, and separate once the radical source is no longer required. While pristine TiO<sub>2</sub> in its anatase form can perform this function, decorating the material enhances free radical generation by a factor of ca. 5, and is attributed to electron trapping by the metallic center that reduces the rate of electron-hole recombination. While we focused on ethers, the rich SED literature suggests that many molecules can perform similarly, as demonstrated here with toluene and acetonitrile. Numerous molecules should be capable of donating an electron to the VB hole, thus being excellent candidates for a remarkable clean and efficient source of free radicals.

## ASSOCIATED CONTENT

**Supporting Information.** SI available free of charge on the ACS Publications website. Experimental and computational methodologies, additional kinetic information, EPR trapping data, MS spectra of the products.

## Corresponding Authors

\*E-mail: jscaiano@uottawa.ca (J.C.S.)

\*E-mail: anabel.lanterna@icloud.com (A.E.L.)

## ACKNOWLEDGMENT

This work was supported by the Natural Sciences and Engineering Research Council of Canada, the Canada Foundation for Innovation, the Canada Research Chairs Program, Canada's International Development Research Centre (IDRC) and the German National Academy of Sciences Leopoldina (Grant No. LPDS 2017-15 to P.C.).

## REFERENCES

- Yi, H.; Zhang, G. T.; Wang, H. M.; Huang, Z. Y.; Wang, J.; Singh, A. K.; Lei, A. W., Recent Advances in Radical C-H Activation/Radical Cross-Coupling. *Chem. Rev.* **2017**, *117* (13), 9016-9085.
- Zhang, S. Y.; Zhang, F. M.; Tu, Y. Q., Direct Sp(3) alpha-C-H activation and functionalization of alcohol and ether. *Chem. Soc. Rev.* **2011**, *40* (4), 1937-1949.
- Taylor, R. D.; MacCoss, M.; Lawson, A. D. G., Rings in Drugs. *J. Med. Chem.* **2014**, *57* (14), 5845-5859.
- Martins, P.; Jesus, J.; Santos, S.; Raposo, L. R.; Roma-Rodrigues, C.; Baptista, P. V.; Fernandes, A. R., Heterocyclic Anticancer Compounds: Recent Advances and the Paradigm Shift towards the Use of Nanomedicine's Tool Box. *Molecules* **2015**, *20* (9), 16852-16891.

- Jin, J.; MacMillan, D. W. C., Direct alpha-Arylation of Ethers through the Combination of Photoredox-Mediated C-H Functionalization and the Minisci Reaction. *Angew. Chem. Int. Edit.* **2015**, *54* (5), 1565-1569.
- Shaw, M. H.; Twilton, J.; MacMillan, D. W. C., Photoredox Catalysis in Organic Chemistry. *J. Org. Chem.* **2016**, *81* (16), 6898-6926.
- Mayer, J. M., Understanding Hydrogen Atom Transfer: From Bond Strengths to Marcus Theory. *Acc. Chem. Res.* **2011**, *44* (1), 36-46.
- Gaya, U. I.; Abdullah, A. H., Heterogeneous photocatalytic degradation of organic contaminants over titanium dioxide: A review of fundamentals, progress and problems. *J. Photochem. Photobio., C: Photochem. Rev.* **2008**, *9* (1), 1-12.
- Morsella, M.; d'Alessandro, N.; Lanterna, A. E.; Scaiano, J. C., Improving the Sunscreen Properties of TiO<sub>2</sub> through an Understanding of Its Catalytic Properties. *ACS Omega* **2016**, *1* (3), 464-469.
- Sendra, M.; Sanchez-Quiles, D.; Blasco, J.; Moreno-Garrido, I.; Lubian, L. M.; Perez-Garcia, S.; Tovar-Sanchez, A., Effects of TiO<sub>2</sub> nanoparticles and sunscreens on coastal marine microalgae: Ultraviolet radiation is key variable for toxicity assessment. *Environ. Int.* **2017**, *98*, 62-68.
- Hanigan, D.; Truong, L.; Schoepf, J.; Nosaka, T.; Mulchandani, A.; Tanguay, R. L.; Westerhoff, P., Trade-offs in ecosystem impacts from nanomaterial versus organic chemical ultraviolet filters in sunscreens. *Water Res.* **2018**, *139*, 281-290.
- Tyagi, A.; Yamamoto, A.; Kato, T.; Yoshida, H., Bifunctional property of Pt nanoparticles deposited on TiO<sub>2</sub> for the photocatalytic sp(3)-C-sp(3)C cross-coupling reactions between THF and alkanes. *Catal. Sci. Technol.* **2017**, *7* (12), 2616-2623.
- Marina, N.; Lanterna, A. E.; Scaiano, J. C., Expanding the Color Space in the Two-Color Heterogeneous Photocatalysis of Ullmann C-C Coupling Reactions. *ACS Catal.* **2018**, *8* (8), 7593-7597.
- Fuchigami, T.; Fuchigami, T. a., Fundamentals and Applications of Organic Electrochemistry: Synthesis, Materials, Devices. Wiley: Hoboken, 2014.
- Schneider, J.; Bahnemann, D. W., Undesired Role of Sacrificial Reagents in Photocatalysis. *Journal of Physical Chemistry Letters* **2013**, *4* (20), 3479-3483.
- Wang, B.; Durantini, J.; Nie, J.; Lanterna, A. E.; Scaiano, J. C., Heterogeneous Photocatalytic Click Chemistry. *J. Am. Chem. Soc.* **2016**, *138* (40), 13127-13130.
- Hernandez Mejia, C.; van Deelen, T. W.; de Jong, K. P., Activity enhancement of cobalt catalysts by tuning metal-support interactions. *Nat Commun* **2018**, *9* (1), 4459.
- Malatesta, V.; Scaiano, J. C., Absolute Rate Constants for the Reactions of Tert-Butoxyl with Ethers - Importance of the Stereoelectronic Effect. *J. Org. Chem.* **1982**, *47* (8), 1455-1459.
- Hainer, A. S.; Hodgins, J. S.; Sandre, V.; Vallieres, M.; Lanterna, A. E.; Scaiano, J. C., Photocatalytic Hydrogen Generation Using Metal-Decorated TiO<sub>2</sub>: Sacrificial Donors vs True Water Splitting. *ACS Energy Lett.* **2018**, *3* (3), 542-545.
- Ciriano, M. V.; Korth, H. G.; van Scheppingen, W. B.; Mulder, P., Thermal stability of 2,2,6,6-tetramethylpiperidine-1-oxyl (TEMPO) and related N-alkoxyamines. *J. Am. Chem. Soc.* **1999**, *121* (27), 6375-6381.
- Orlov, Y. D.; Chernova, E. M.; Turovtsev, V. V., Enthalpies of formation of organic free radicals of alcohol and ether derivatives. *Russ. Chem. Bull.* **2010**, *59* (10), 2009-2013.
- Giannozzi, P.; Baroni, S.; Bonini, N.; Calandra, M.; Car, R.; Cavazzoni, C.; Ceresoli, D.; Chiarotti, G. L.; Cococcioni, M.; Dabo, I.; Dal Corso, A.; de Gironcoli, S.; Fabris, S.; Fratesi, G.; Gebauer, R.; Gerstmann, U.; Gougoussis, C.; Kokalj, A.; Lazzeri, M.; Martin-Samos, L.; Marzari, N.; Mauri, F.; Mazzarello, R.; Paolini, S.; Pasquarello, A.; Paulatto, L.; Sbraccia, C.; Scandolo, S.; Sclauzero, G.; Seitsonen, A. P.; Smogunov, A.; Umari, P.; Wentzcovitch, R. M., QUANTUM ESPRESSO: a modular and open-source software project for quantum simulations of materials. *J. Phys.: Condens. Matter* **2009**, *21* (39).
- Holmes, J. L.; Lossing, F. P.; Mayer, P. M., The Effects of Methyl Substitution on the Structure and Thermochemistry of the Cyanomethyl Radical and Cation. *Chem. Phys. Lett.* **1993**, *212* (1-2), 134-140.
- De Vleeschouwer, F.; Van Speybroeck, V.; Waroquier, M.; Geerlings, P.; De Proft, F., Electrophilicity and nucleophilicity index for radicals. *Org. Lett.* **2007**, *9* (14), 2721-2724.

# Toc Graphic

